A candidate $LiBH_4$ for hydrogen storage: Crystal structures and reaction mechanisms of intermediate phases

Jeung Ku Kang[a] and Se Yun Kim
Department of Materials Science and Engineering, KAIST, Daejeon 305-701, Republic of Korea

Young Soo Han
LG Electronics, Institute of Technology, Devices and Materials Laboratory, Seoul 137-724, Republic of Korea

Richard P. Muller
Computational Materials and Molecular Biology, Sandia National Laboratories, Albuquerque, New Mexico 87185-0996

William A. Goddard III
Materials and Process Simulation Center, California Institute of Technology, Pasadena California 91125-7400

(Received 17 December 2004; accepted 4 August 2005; published online 6 September 2005)

First-principles calculation and x-ray diffraction simulation methods have been used to explore crystal structures and reaction mechanisms of the intermediate phases involved in dehydriding of $LiBH_4$. $LiBH_4$ was found to dehydride via two sequential steps: first dehydriding through LiBH, followed by the dehydriding of LiBH through LiB. The first step, which releases 13.1 wt. % hydrogen, was calculated to have an activation barrier of 2.33 eV per formula unit and was endothermic by 1.28 eV per formula unit, while the second step was endothermic by 0.23 eV per formula unit. On the other hand, if $LiBH_4$ and LiBH each donated one electron, possibly to the catalyst doped on their surfaces, it was found that the barrier for the first step was reduced to 1.50 eV. This implies that the development of the catalyst to induce charge migration from the bulk to the surface is essential to make $LiBH_4$ usable as a hydrogen storage material in a moderate temperature range, which is also important to stabilize the low-temperature structure of *Pnma* (no. 62) LiBH on dehydrogenation. Consequently, the high 13.1 wt. % hydrogen available from the dehydriding of $LiBH_4$ and LiBH and their phase stability on *Pnma* when specific catalysts were used suggest that $LiBH_4$ has good potential to be developed as the hydrogen storage medium capable of releasing the Department of Energy target of 6.5 wt. % for a hydrogen fuel cell car in a moderate temperature range. © *2005 American Institute of Physics*. [DOI: 10.1063/1.2042632]

There is great interest in small and lightweight hydrogen storage materials.[1,2] Hydrogen fuel, which can be produced from renewable energy sources, contains a much larger chemical energy per mass (142 MJ kg^{-1}) than any hydrocarbon fuel, thus making a hydrogen fuel cell an attractive alternative to the internal combustion engine for transportation. A hydrogen fuel cell car needs to store at least 4 kg hydrogen to cover the same range as a gasoline-powered car.[1] On the other hand, to store this hydrogen at room temperature and atmospheric pressure requires such a large volume that corresponds to a balloon with a 4.5 m diameter, which is hardly a practical volume for a small vehicle. To reduce this problem, one could consider using liquid hydrogen for hydrogen storage since it has a high mass density[1] (70.8 kg m^{-3}). However, to liquefy hydrogen requires expensive processes due to its low condensation temperature[1] (−252 °C at 1 bar). An additional problem is that heat transfer through the available modern containers can result in a loss of up to 40% of the energy content in hydrogen.[3] Currently, in this respect, there is much interest in storing hydrogen on advanced carbons and lightweight metals. Dillon *et al.*[4] reported that 6–8 wt. % hydrogen was stored in single-walled nanotubes (SWNTs). However, controversial results[5,6] have been reported concerning the true hydrogen storage capacity on advanced carbons. Hirscher and his coworkers[5] argued against Dillon's report by showing that titanium hydrides in the SWNT stored large amounts of hydrogen, but the hydrogen storage capacity on SWNT itself was less than 1 wt. %. Likewise, Chen *et al.*[6] showed that the increase in the hydrogen storage capacity by alkaline metal-doped carbon NTs was attributed to the formation of metal hydrides. Putting all of these results together, one could say that the reversible hydrogen content on the pristine SWNT still does not satisfy the Department of Energy (DOE) target[1] of 6.5 wt. %.

A promising alternative for hydrogen storage is the metal hydride system. However, there are still considerable challenges to meet the requirements[1,7] for practical applications that include (1) increasing the maximum weight percent of reversible hydrogen to 6.5 wt. %, (2) increasing the maximum hydrogen capacity per volume to 62 kg m^{-3}, and (3) improving the rate for adsorption/desorption to 1–3 g s^{-1}. In the search for metal hydrides with higher than hitherto known gravimetric storage capacities, $LiBH_4$, with light elements Li and B, has been considered for this purpose due to its high available 18.5 wt. % hydrogen. The recent experimental x-ray diffraction (XRD) study[8] and theoretical predictions by Miwa *et al.*[9] and Ge *et al.*[10] indicate that $LiBH_4$ is the most stable when it has orthorhombic symmetry. On the other hand, detailed knowledge about the mechanisms of re-

[a]Electronic mail: jeungku@kaist.ac.kr

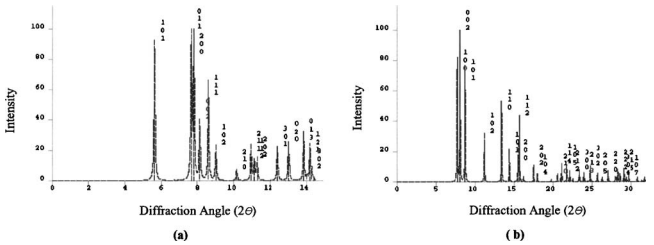

FIG. 1. Simulated XRDs from *Pnma* and $P6_3mc$ $LiBH_4$ at the wavelengths $\lambda=0.486$ Å and $\lambda=0.949$ Å, respectively: (a) *Pnma* and (b) $P6_3mc$. Diffraction angles are 2θ values.

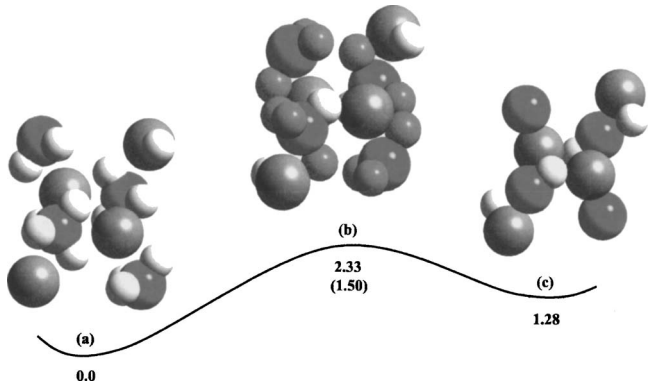

FIG. 2. (Color online) Intermediate structures involved in dehydriding of $LiBH_4$. (a) $LiBH_4$, (b) the transition state connecting $LiBH_4$ to LiBH, and (c) LiBH. Li and B atoms are shown in dark gray and green, respectively, while H atoms except desorbing H atoms in blue are shown in white. Energies (eV) per formula unit are not to scale, where the barrier in parenthesis is determined from their ionized structures.

moving hydrogen and adding hydrogen has not yet been reported. However, we consider that this knowledge can be obtained by using density functional theory (DFT)[11,12] calculations, as they allow accurate determination of crystal structures and their energies.

All calculations were performed on the PW91 method[13] using Vanderbilt pseudopotentials[14] with a cutoff energy of 270 eV. First, we considered the B32 (Fd-3m) structure for LiB and perform the total energy calculations using 270 eV (9880 k-points) and 300 eV cutoff energy (37 671 k-points). Their total energies per formula unit were found to differ by only 2.51 kJ/mol, which indicates that the 270 eV cutoff energy is somehow optimal in terms of both being able to reduce the considerably expensive computational cost by using much larger cutoff energies and also being reasonably accurate in their total energies. The set of k-points used to expand the wave functions was based on the Monkhorst-Pack scheme.[15] In addition, we used Gillan's thermal broadening scheme[16] with broadening energies of 0.2 eV. All electronic structure calculations for optimizing geometries were carried out using the CASTEP[17] program, and simulated XRD[18] patterns were determined through simulations of d-spacing, 2θ, and intensities for hkl reflections at the optimized geometries.

First, we determined the lowest-energy structure for LiB through geometry optimizations of several types: namely, the Fd-3m, $I4_1/a$, *Pnma*, $Cmc2_1$, $P6_3mc$, and $P2_1/c$ space group types. The *Pnma* structure is determined as the lowest-energy structure for LiB, with the $P2_1/c$ structure 0.39 eV, the $Cmc2_1$ structure 0.83 eV, the Fd-3m structure 1.14 eV, the $I4_1/a$ structure 2.82 eV, and the $P6_3mc$ structure 4.38 eV per formula unit higher. The optimized lattice parameters for *Pnma* LiB are obtained as $a=6.41$ Å, $b=3.01$ Å, and $c=5.60$ Å with $\alpha=90.0°$, $\beta=90.0°$, and $\gamma=90.0°$, in which the B–B distance of 1.52 Å and the B–B–B angle of 165.0° suggest that the B–B bonding has a certain character of sp hybridization.

$LiBH_4$ consists of BH_4^- anions spaced by Li^+ counter ions. As an initial guess for $LiBH_4$, we used the Fd-3m $LiBH_4$ structure, but its simulated XRD was found to disagree with the experimental hkl reflections.[8] The hkl reflections from $I4_1/a$ $LiBH_4$ were also predicted to disagree with experimental hkl reflections. On the other hand, the simulated XRD [see Fig. 1(a)] peaks at the wavelength $\lambda=0.486$ Å from orthorhombic $LiBH_4$ [Fig. 2(a)] were found to agree with the experimental patterns. The strongest XRD peak was (011) with $2\theta=7.66°$, and the ratio of the second strongest (101) peak with $2\theta=5.63°$ to the strongest peak was 92.26%, while the third strongest (200) peak with $2\theta=7.80°$ had a ratio of $I(200)/I(011)=83.41\%$. The *Pnma* structure was the lowest-energy structure for $LiBH_4$ having predicted lattice parameters of $a=7.14$ Å, $b=4.29$ Å, and $c=6.85$ Å with $\alpha=90.0°$, $\beta=90.0°$, and $\gamma=90.0°$, which compared to experimental values:[8] $a=7.18$ Å, $b=4.44$ Å, and $c=6.80$ Å with $\alpha=90.0°$, $\beta=90.0°$, and $\gamma=90.0°$ (see Table I). For *Pnma* $LiBH_4$, each B had four H tetrahedrally coordinated to form BH_4^- with the B–H bond distance of 2.21 to 2.22 Å and the H–B–H bond angle of 109.3° to 110.6°, while the Li–H distance was 2.05 to 2.13 Å. Additionally, the total energies for $Cmc2_1$, $P6_3mc$, and $P2_1/c$ $LiBH_4$ were determined through full geometry optimizations, but the $Cmc2_1$ structure was 2.13 eV, the $P6_3mc$ structure was 0.31 eV, and the $P2_1/c$ structure was 0.16 eV per formula unit energetically less stable than the *Pnma* $LiBH_4$.

We also determined energies and structures for the plausible intermediate phases such as Li_3BH_6, $LiBH_2$, LiBH, and LiB. Li_3BH_6 is described in terms of three Li^+ ions surrounding each $[BH_6]^{-3}$ molecule (see Table II). We found that Li_3BH_6 was the most stable in the R-3 phase, but that the dehydriding of $LiBH_4$ through Li_3BH_6 was endothermic by 3.57 eV per formula unit, while those through the lowest-energy structures of *Pnm* LiBH and *Pnma* $LiBH_2$ were endothermic by 1.28 and 2.89 eV, respectively, per formula unit. Thus, these results suggest that the dehydriding of $LiBH_4$ through LiBH is the most preferable reaction. The reaction barrier of 2.33 eV per formula unit for the dehydriding of $LiBH_4$ to LiBH was also obtained from the geometries, as seen in Fig. 2, where the H–H bond distance for a desorbing H_2 is 1.463 Å. However, it should be noted that a high temperature (>400 K) would be needed to obtain a practical amount of released hydrogen from $LiBH_4$ due to its relatively high barrier of 2.33 eV. On the other hand, the low-temperature structure of *Pnma* LiBH might be unstable at this high temperature. Consequently, dehydrogenation of $LiBH_4$ and hydrogenation of LiBH should be "reversible" only if the dehydrogenation temperature could be reduced to the extent that *Pnma* LiBH is stabilized. The recent experimental study by Vajo *et al.*[19] showed that $LiBH_4$ could be developed as reversible hydrogen storage when specific catalysts were used. We also found that the barrier was reduced to 1.50 eV when $LiBH_4$ donated one electron, possibly to the catalyst doped on the hydrogen storage material surface, where the H–H bond distance of a desorbing H_2 is 1.159 Å.

TABLE I. Atomistic details and energies per formula unit for the lowest-energy structures of $LiBH_4$, Li_3BH_6, $LiBH_2$, LiBH, and LiB from this work.

Phase	Atomic Coordinates ($x/a, y/b, z/c$)	Lattices a,b,c(Å)α,β,γ(°)	Energy (eV)
$LiBH_4$[a]	Li: (0.16 0.25 010), B: (0.30 0.25 0.42) H: (0.91 0.25 0.94), (0.39 0.25 0.27), (0.20 0.02 0.42)	a=7.1 b=4.3 c=6.9 $\alpha=\beta=\gamma$=90	−333.816[b]
Li_3BH_6[c]	Li: (0.95 0.22 0.31), B: (0.00 0.00 0.00), (0.00 0.00 0.50) H: (0.85 0.83 0.10), (0.65 0.48 0.43)	$a=b$=7.4 c=8.8 $\alpha=\beta$=90, γ=120	−744.316
$LiBH_2$[a]	Li: (0.24 0.25 0.14), B: (0.45 0.25 0.42) H: (0.07 0.25 0.94), (0.51 0.25 0.23)	a=8.1, b=3.0 c=5.9 $\alpha=\beta=\gamma$=90	−299.208
LiBH[a]	Li: (0.24 0.25 0.21) B: (0.45 0.25 0.51) H: (0.75 0.25 0.96)	a=6.2, b=3.0, c=6.3 $\alpha=\beta=\gamma$=90	−284.979
LiB[a]	Li: (0.26 0.25 0.24) B: (0.50 0.25 0.52)	a=6.4 b=3.0 c=5.6 $\alpha=\beta=\gamma$=90	−268.901

[a]Orthorhombic phase *Pnma* (space group of no. 62). Total energies per formula unit of other space group types for $LiBH_4$ are also given: $P2_1/c$(−333.656 eV), $P6_3mc$ (−333.514 eV), $I4_1/a$ (−333.154 eV), Fd-3m (−332.577 eV), and $Cmc2_1$ (−331.687 eV).
[b]Reaction energy calculated without zero-point and thermal corrections.
[c]Hexagonal phase R-3 (space group of no. 148).

The 1.50 eV barrier was compared to the 1.62 eV obtained experimentally from SiO_2-catalyzed $LiBH_4$ by Zuttel and his co-workers.[20] In this respect, we can conclude that the development of the catalyst to induce charge migration from the bulk to the surface is essential to lower the activation barrier and the temperature for dehydrogenation of $LiBH_4$, thus also to stabilize *Pnma* LiBH on dehydrogenation. Moreover, another good finding was that the 13.1 wt. % hydrogen was available from dehydriding of $LiBH_4$ through LiBH.

In summary, metal hydride systems such as $LiAlH_4$ and $NaAlH_4$[21,22] with high hydrogen storage capacities are suffering from formation of intermediate structures having different phases on dehydrogenation, which results in slow kinetics on dehydrogenation. In this respect, the phase stability of $LiBH_4$ and LiBH on the *Pnma* structure when specific catalysts were used and the 13.1 wt. % hydrogen available from dehydriding of $LiBH_4$ to LiBH are very important aspects. Consequently, we conclude that the catalyst-doped $LiBH_4$ could be a very attractive hydrogen storage material capable of releasing the DOE target[1] of 6.5 wt. % for a hydrogen fuel cell car in a moderate temperature range.

TABLE II. Summary of reaction energies and barriers per formula unit from this work.

Reaction	Energy (eV)	Barrier (eV)
Thermal decomposition of $LiBH_4$		
$LiBH_4$[a]$\rightarrow(1/3)Li_3BH_6$[b]$+(2/3)$B[c]$+H_2$	3.57[d]	
$LiBH_4$[a]$\rightarrow$LiBH[a]$+(3/2)H_2$	1.28[d]	2.33 (1.50)[e]
Thermal decomposition of LiBH		
LiBH[a]$\rightarrow$LiB[a]$+(1/2)H_2$	0.23[d]	

[a]Orthohombic phase *Pnma* (space group of no. 62).
[b]Hexagonal phase R-3 (space group of no. 148).
[c]Face-centered cubic lattice.
[d]Reaction energy calculated without zero-point and thermal corrections.
[e]Reaction barrier calculated without zero-point and thermal corrections. The value in parenthesis is the barrier determined from the ionized unit cells.

This research was supported by General Motors Global Alternative Proposal Center.

[1] L. Schlapbach and A. Züttel, Nature (London) **414**, 353 (2001).
[2] J. Pettersson and O. Hjortsberg, Hydrogen Storage Alternatives: A Technological and Economic Assessment (KFB-Meddelande, Stockholm, 1999:27), http://www.kfb.se/pdfer/M-99-27.pdf
[3] D. Hart, Storing and Transporting Hydrogen (E-sources, London, 1998), http://www.e-sources.com/hydrogen/storage.html
[4] A. C. Dillon, K. M. Jones, T. A. Bekkedahl, C. H. Kiang, D. S. Bethune, and M. J. Heben, Nature (London) **386**, 377 (1997).
[5] M. Hirscher, M. Becher, M. Haluska, U. Dettlaff-Weglikowska, A. Quintel, G. S. Duesberg, Y.-M. Choi, P. Downes, M. Hulman, S. Roth, I. Stepanek, and P. Bernier, Appl. Phys. A: Mater. Sci. Process. **72**, 129 (2001).
[6] P. Chen, X. Wu, J. Lin, and K. L. Tan, Science **285**, 91 (1999).
[7] G. D. Berry and S. M. Aceves, Energy Fuels **12**, 49 (1998).
[8] J-Ph. Soulié, G. Renaudin, R. Černý, and K. Yvon, J. Alloys Compd. **346**, 200 (2002).
[9] K. Miwa, N. Ohba, S. I. Towata, Y. Nakamori, and S. I. Orimo, Phys. Rev. B **69**, 245120 (2004).
[10] Q. Ge, J. Phys. Chem. A **108**, 8682 (2004).
[11] P. Hohenberg and W. Kohn, Phys. Rev. **136**, B864 (1964).
[12] W. Kohn and L. J. Sham, Phys. Rev. **140**, A1133 (1965).
[13] J. P. Perdew and Y. Wang, Phys. Rev. B **45**, 13244 (1992).
[14] D. Vanderbilt, Phys. Rev. B **41**, 7892 (1990).
[15] H. J. Monkhorst and J. D. Pack, Phys. Rev. B **13**, 5188 (1976).
[16] M. J. Gillan, J. Phys.: Condens. Matter **1**, 689 (1989).
[17] M. C. Payne, M. P. Teter, D. C. Allan, T. A. Arias, and J. D. Joannopoulos, Rev. Mod. Phys. **64**, 1045 (1992).
[18] A. J. Howard, G. L. Gilliland, B. C. Finzel, T. L. Poulos, D. H. Ohlendorf, and F. R. Salemme, J. Appl. Crystallogr. **20**, 383 (1987).
[19] J. J. Vajo, S. L. Skeith, and F. Mertens, J. Phys. Chem. B **109**, 3719 (2005).
[20] A. Zuttel, S. Rentsch, P. Fischer, P. Wenger, P. Sudan, and C. Emmenegger, J. Alloys Compd. **356**, 515 (2003).
[21] J. Chen, N. Kuriyama, Q. Xu, H. T. Takeshita, and T. Sakai, J. Phys. Chem. B **105**, 11214 (2001).
[22] J. K. Kang, J. Y. Lee, R. P. Muller, and W. A. Goddard III, J. Chem. Phys. **121**, 10623 (2004).